

Dielectric Constants and Crystal Structures of CaYAlO_4 , CaNdAlO_4 , and SrLaAlO_4 , and Deviations from the Oxide Additivity Rule

R. D. SHANNON, R. A. OSWALD, AND J. B. PARISE*

*Central Research and Development, † E. I. du Pont de Nemours & Co.,
Experimental Station, Wilmington, Delaware 19880-0356*

B. H. T. CHAI

*Department of Physics and Mechanical Engineering, Center for Research on
Electrooptics and Lasers, University of Central Florida, 12424 Research
Parkway, Suite 400, Orlando, Florida 32826*

P. BYSZEWSKI AND A. PAJACZKOWSKA

*Institute of Physics, Polish Academy of Sciences, Al. Lotnikow 32/46,
Pl-02688 Warszawa, Poland*

AND R. SOBOLEWSKI‡

*Department of Electrical Engineering and Laboratory for Laser Energetics,
University of Rochester, Rochester New York 14627*

Received September 16, 1991

The structures of CaYAlO_4 , CaNdAlO_4 , and SrLaAlO_4 have been refined using single-crystal X-ray diffraction data. These compounds possess the full symmetry of the K_2NiF_4 structure type, $I4/mmm$, with lattice parameters $a = 3.6451(1)$ and $c = 11.8743(6)$ Å for CaYAlO_4 , $a = 3.6847(3)$ and $c = 12.124(2)$ Å for CaNdAlO_4 , and $a = 3.7564(1)$ and $c = 12.6357(5)$ Å for SrLaAlO_4 . Inspection of the interatomic distances reveals stretching of the Al-O bond, from an average of 1.878 to 1.901 to 1.935 Å, as smaller cations (CaY) are replaced by larger cations (CaNd) and (SrLa) in the MM' sites between the two dimensional aluminate sheets. The dielectric constants (κ') and dielectric loss values of CaYAlO_4 , CaNdAlO_4 , and SrLaAlO_4 were measured at 1 MHz using a two-terminal method with empirically determined edge corrections. The results are

CaYAlO_4	$\kappa'_a = 21.44 \pm .02$	$\tan \delta_a = 0.0008$
	$\kappa'_c = 16.12 \pm .04$	$\tan \delta_c = 0.0008$
CaNdAlO_4	$\kappa'_a = 19.65 \pm .1$	$\tan \delta_a = 0.0002$
	$\kappa'_c = 17.65 \pm .1$	$\tan \delta_c = 0.0004$

* Present address: Mineral Physics Institute, Earth and Space Sciences Bldg., State University of New York, Stony Brook, NY 117794-2100.

† Contribution No. 6007.

‡ Also at the Institute of Physics, Polish Academy of Sciences, Al. Lotnikow 32/46, PL-02668 Warszawa, Poland.

SrLaAlO₄

$$\kappa'_a = 16.81 \pm .1$$

$$\kappa'_c = 20.02 \pm .1$$

$$\tan \delta_a = 0.0006$$

$$\tan \delta_c = 0.0008.$$

The deviations of measured dielectric polarizabilities, as determined from the Clausius–Mosotti equation and those calculated from the sum of oxide polarizabilities according to $\alpha_D(MM'AlO_4) = \alpha_D(MO) + 0.5 \alpha_D(M'_2O_3) + 0.5 \alpha_D(Al_2O_3)$, are +1.7% for CaYAlO₄, –2.0% for CaNdAlO₄, and –5.9% for SrLaAlO₄. The deviations from additivity are believed to result from K₂NiF₄ structural constraints leading to “rattling” *M* and *M'* ions in CaYAlO₄ and “compressed” *M* and *M'* ions in CaNdAlO₄ and SrLaAlO₄. © 1992 Academic Press, Inc.

Introduction

The concept of additivity of molecular polarizabilities, whereby the molecular polarizability of a complex substance can be broken up into the molecular polarizabilities of simpler substances according to

$$\alpha_D(M_2M'X_4) = 2 \alpha_D(MX) + \alpha_D(M'X_2),$$

has been discussed (1–7). We recently evaluated the validity of the oxide additivity rule in several Y and rare earth aluminate garnets, the minerals chrysoberyl, spinel, phenacite, forsterite, and danburite, zircon, olivine-type silicates, and a group of beryllates, borates, and phosphates and found agreement between calculated and observed polarizabilities of 0.5–1.5% (8–14). However, crystallographically constrained structures such as the silicate garnets of the type X₃Al₂Si₃O₁₂ lead to large deviations from additivity when the X–O bond distances are unusually large (*X* = Mg) or unusually small (*X* = Ca) (15). It is of interest to see whether other compounds with constrained structures exhibit the same behavior. Compounds such as MM'AlO₄ with K₂NiF₄ structure fall in this category. These compounds are also of interest because of their application as substrates for high-*T*_c thin films (16, 17). The purpose of this paper is to determine the crystal structures and dielectric constants of CaYAlO₄, CaNdAlO₄, and SrLaAlO₄, and to evaluate the validity of the oxide additivity rule in these MM'AlO₄ compounds.

Experimental

Single crystals of CaYAlO₄ were grown using the Czochralski technique similar to that of Appen *et al.* (18, 19). A charge with the stoichiometry Ca : Y : Al = 1 : 1 : 1 using 99.999% purity oxides was loaded into an Ir crucible and heated inductively in a pure N₂ atmosphere. The seed crystal was produced by spontaneous nucleation on an Ir wire. An [001]-oriented seed was used to produce a crystal of 25 mm diameter using a pull rate of 2 mm/hr. The crystal had a brownish-yellow color similar to that reported earlier (18, 19). The color may result from a slight Ca : Y nonstoichiometry. Although Appen *et al.* (18) reported that the color could be bleached out by annealing at 1200°C for 5 hr at low oxygen pressures (<1 Pa), this technique was not successful in reducing the coloration of our crystals. These crystals show a pronounced cleavage parallel to (001) which causes difficulties in crystal growth and wafer fabrication of LaSrAlO₄. This cleavage problem is much less serious for CaYAlO₄, allowing easy growth of [001]-oriented seeds and 0.5-mm-thick wafers to be prepared without difficulty. Domain structures which were occasionally seen appeared to be related to pull and rotation rates. CaYAlO₄ appears to be easier to grow than SrLaAlO₄ but its smaller *a*-axis seems to be detrimental to film performance.

Crystals of both CaNdAlO₄ and SrLaAlO₄ were grown by the Czochralski technique. The compounds were prepared from 4*N* pu-

rity Nd_2O_3 , Al_2O_3 , CaCO_3 , and La_2O_3 . The mixed powders were melted in an inductively heated 36-mm-diameter Ir crucible in N_2 with 1% O_2 and homogenized for 2–3 hr before the seed was immersed. Both CaNdAlO_4 and SrLaAlO_4 melted congruently at about 1820 and 1650°C, respectively. In the early runs (16, 20), the crystals were grown from stoichiometric melts with a flat crystal-melt growth interface. However, the resulting crystals were sometimes cracked. Our later studies (21) showed that both CaNdAlO_4 and SrLaAlO_4 had a tendency for strongly anisotropic growth with preferential (101) growth planes. The crystals used in this study were grown according to the procedure in Ref. (21). The crystal rotation speed and melt temperature gradient were adjusted in such a way that the convex surface formed by the (101) planes could be maintained throughout the entire growth. We used nonstoichiometric melts with up to 7 mole% excess CaO and 2 mole% SrO for CaNdAlO_4 and SrLaAlO_4 , respectively. The excess CaO and SrO stabilized the melts and resulted in crystals free of inclusion and cracks.

Electron microprobe analyses were made using a JEOL 733 electron microprobe. Data reduction methods are described by Armstrong (22, 23), who states that the mean relative errors of the analyses are generally 1% or lower for silicates but somewhat higher for samples with average atomic numbers higher than those found in silicates due to uncertainties in the absorption and fluorescence correction factors used for the less common elements. Analyses of nominally CaNdAlO_4 and SrLaAlO_4 gave $\text{Ca}_{0.984}\text{Nd}_{0.987}\text{Al}_{1.022}\text{O}_4$ and $\text{Sr}_{0.976}\text{La}_{0.980}\text{Al}_{1.029}\text{O}_4$. A recognized interference between the rare earth elements and Al makes the Al values about 4% higher than what is believed to be the true value. Because the exact magnitude of the correction is currently unknown, the results are presented as determined without correction for this

effect. For the purposes of this investigation we assume the compounds to have stoichiometric $MM'\text{AlO}_4$ compositions.

Single-crystal X-ray diffraction data were collected on an Enraf-Nonius CAD-4 diffractometer using the experimental parameters given in Table I. Crystals were cut with faces parallel to the {100} forms in order to facilitate the analytical absorption corrections performed for each data set. The cell parameters (Table I) were determined from 25 reflections with $12^\circ < 2\theta < 46^\circ$. The X-ray diffraction patterns of CaYAlO_4 and SrLaAlO_4 were obtained on a Guinier-type focusing camera using $\text{CuK}\alpha_1$ radiation and Si SRM 640 internal standard. Data were corrected for Lorentz and polarization effects. Samples were subjected to a second harmonic generation test, which proved negative, suggesting the space group was indeed centric. We were unable to verify the Byszewski *et al.* (24) $I4mm$ space group which was based on observed powder X-ray diffraction intensities and implies ordering of MM' cations. Structure refinement for each sample was initiated using the starting parameters for the K_2NiF_4 structure using a set of programs developed by J. C. Calabrese (25). The final refinement employed an anisotropic model for the thermal motion of all atoms; the discrepancy indices reported in Table I were obtained. The refined atomic parameters and selected bond lengths are given in Tables II and III, respectively.

Rectangular-shaped samples having areas ranging from 0.18 to 0.56 cm^2 and thicknesses from 0.05 to 0.14 cm, prepared according to the technique described earlier (28), were used to measure the dielectric constant. Dielectric constant measurements were performed over the frequency range 30 KHz–3 MHz with a parallel plate capacitance technique using Hewlett-Packard 4274A and 4275A LCR bridges and fixture 16034B (Test Tweezers) (29). Details of the experimental procedure were published pre-

TABLE I
 SUMMARY OF X-RAY DIFFRACTION DATA FOR $MM'AlO_4$

	CaYAlO ₄	CaNdAlO ₄	SrLaAlO ₄
Space group		<i>I4/mmm</i>	
<i>a</i> (Å)	3.6451(1) ^a	3.6847(3)	3.7564(1) ^a
<i>c</i> (Å)	11.8743(6)	12.124(2)	12.6357(5)
Temperature (°C)		20	
Volume (Å ³)	157.77	164.61	178.30
<i>Z</i>		2	
Formula weight	219.97	275.30	317.51
Calculated density (g/cm ³)	4.640	5.553	5.926
μ (Mo) (cm ⁻¹)	203.44	174.76	265.50
Diffractometer		Enraf-Nonius CAD4	
Radiation		MoK α	
Data collected	1404	4056	2396
Minimum and maximum 2θ (°)	7–70	4–80	4–70
Maximum $ h $, $ k $, $ l $	5, 5, 18	6, 6, 21	6, 6, 20
Data octants	+++ , ++- , +-+ , -++ , --- , --+ , -+- , ---		
Scan method		$\omega/2\theta$	
Absorption method		Analytical	
Transmission factors (range)	0.04–0.12	0.03–0.16	0.04–0.11
No. of unique data ($I > 3\sigma(I)$)	109	181	139
Refinement method		Full-matrix least-squares on <i>F</i>	
Anomalous dispersion	Ca and Y	Ca and Nd	Sr and La
Weighting scheme	$\propto[\sigma^2(I) + 0.009I^2]^{-1/2}$	$\propto[\sigma^2(I) + 0.008I^2]^{-1/2}$	$\propto[\sigma^2(I) + 0.008I^2]^{-1/2}$
Atoms refined		All anisotropic	
Parameters varied		13	
Parameter/data ratio	8.38	13.92	10.69
<i>R</i>	0.0365	0.0250	0.0187
<i>R_w</i>	0.0362	0.0374	0.0214
Error of fit	1.67	2.08	1.19
Second extinction, (mm × 10 ⁻⁴)	0.34(4)	0.33(3)	0.30(2)

^a Cell dimensions from least-squares refinement of Guinier X-ray data.

 TABLE II
 FINAL REFINED ATOMIC POSITIONAL (× 10⁴) AND EQUIVALENT ISOTROPIC THERMAL (Å²) PARAMETERS FOR $MM'AlO_4$ MATERIALS IN SPACE GROUP *I4/mmm*^a

A-site for ($MM'AlO_4$) ^b	<i>z</i> (A)	<i>z</i> (O2)	<i>B</i> (A)	<i>B</i> (Al)	<i>B</i> (O1)	<i>B</i> (O2)
CaY	3581.6(8)	1679(6)	0.5(1)	0.4(1)	0.6(1)	1.3(1)
CaNd	3583.6(3)	1665(4)	0.4(1)	0.3(1)	0.2(1)	0.8(1)
LaSr	3588.5(2)	1625(4)	0.4(1)	0.5(1)	0.5(1)	0.9(1)

^a Unit cell parameters are given in Table I.

^b Atomic positions are as follows: MM' site at position 4*e* at (0, 0, *z*); Al at 2*a* ($\frac{1}{2}$, $\frac{1}{2}$, $\frac{1}{2}$); O1 at 4*c* ($\frac{1}{2}$, 0, $\frac{1}{2}$), and O2 at 4*e* (0, 0, *z*).

TABLE III
SELECTED INTERATOMIC DISTANCES FOR $MM'AlO_4$
MATERIALS ($MM' = CaY, CaNd, \text{ OR } SrLa$)

Atoms	CaY	CaNd	SrLa
$MM'-O(1) \times 4$	2.4799(7)	2.5186(3)	2.5882(2)
$MM'-O(2)^a \times 4$	2.5936(9)	2.6228(5)	2.6678(5)
$MM'-O(2)$	2.259(7)	2.326(5)	2.480(5)
$\langle MM'-O \rangle$	2.506	2.544	2.612
Ideal ^b	2.528	2.572	2.666
$\delta(MM'-O)^c$	-0.022	-0.028	-0.054
$V_{MM'}$ (v.u.) ^d	2.35	2.36	2.58
Al(1)-O(1) $\times 4$	1.8209(2)	1.84235(5)	1.8768(1)
Al(1)-O(2) ^e $\times 2$	1.992(7)	2.018(4)	2.052(5)
$\langle Al-O \rangle$	1.878	1.901	1.935
Ideal ^b	1.935	1.935	1.935
$\delta(Al-O)^e$	-0.057	-0.034	0.000
V_{Al} (v.u.) ^d	3.32	3.13	2.85

$$^a \frac{1}{2} + X, \frac{1}{2} + Y, \frac{1}{2} - Z.$$

^b Calculated from the sum of the ionic radii for 6-coordinated Al^{3+} (0.535 Å) and O^{2-} (1.40 Å), and 9-coordinated Ca^{2+} (1.18 Å), Y^{3+} (1.075 Å), Nd^{3+} (1.163 Å), Sr^{2+} (1.31 Å), and La^{3+} (1.216 Å) (26).

^c Difference between ideal average and observed average bond distances.

^d $V = \exp[(R_o - R)/0.37]$, where R = observed bond distance; $R_o(MM') = [R_o(M) + R_o(M')]/2$; $R_o(Al) = 1.651$ Å; $R_o(Ca) = 1.967$ Å; $R_o(Sr) = 2.118$ Å; $R_o(Y) = 2.019$ Å; $R_o(Nd) = 2.105$ Å; and $R_o(La) = 2.172$ Å (27).

$$^e \frac{1}{2} + X, \frac{1}{2} + Y, \frac{1}{2} + Z.$$

viously (28). Edge capacitance was calculated from an expression determined empirically from data on standard fused silica, CaF_2 , and SrF_2 ,

$$C_e = (0.019 \ln P/t - 0.043)P,$$

where P and t are sample perimeter and thickness in centimeters. The overall accuracy of the dielectric constant measurements using the above technique is estimated to be 0.5–1.5%. Dielectric loss ($\tan \delta$) errors are estimated to be 5–20% at levels of $\tan \delta = 0.002$ and to be 50–100% at levels of 0.0004–0.0005 (28).

Results

Table IV summarizes the single-crystal dielectric data for $CaYAlO_4$, $CaNdAlO_4$, and $SrLaAlO_4$. $CaYAlO_4$ and $CaNdAlO_4$ showed decreases of less than 0.3% in κ' over the frequency range 30 KHz to 3 MHz, whereas $SrLaAlO_4$ showed a decrease of 0.5% over the same range. The dissipation factors are all less than 0.0010, suggesting good crystal quality and purity. The dissipation factor of $CaNdAlO_4$ is exceptionally low.

All three $MM'AlO_4$ compounds show considerable anisotropy in the dielectric constant which changes as the average relative size of the MM' cations increase. κ'_a decreases whereas κ'_c increases as the average ionic radii of M and M' , $r(M, M')$, increase. The values of κ'_a of $CaNdAlO_4$ and $SrLaAlO_4$ obtained here at 1 MHz (19.65 and 16.81, respectively) agree well with the values obtained by Sobolewski *et al.* (16) at 200–1000 GHz (20 and 17, respectively). The related compound La_2CuO_4 shows anisotropy at 4.2 K similar to that of $CaYAlO_4$ and $CaNdAlO_4$ with saturation values of κ'_a (31) $>$ κ'_c (27) as determined by Chen *et al.* (33) and with values of κ'_a (45) $>$ κ'_c (23) as determined by Reagor *et al.* (34).

Discussion

The structure of the tetragonal $MM'AlO_4$ materials ($MM' = CaY, CaNd, \text{ OR } SrLa$) is of the K_2NiF_4 type illustrated in Fig. 1. The AlO_6 octahedra form a two-dimensional net by corner-shared oxygen atoms. These AlO_3 layers, reminiscent of these found in perovskite, are separated by $(M, M')O$ slabs with the rock salt structure (Fig. 1). The M and M' cations are 9-coordinated to oxygen within this structural unit.

Within the basal plane the Al–O1 bond distance is constrained by the unit cell dimensions since both O1 and Al reside on special positions (see Tables I and II). On

TABLE IV
SUMMARY OF DIELECTRIC CONSTANTS AND TOTAL POLARIZABILITIES

Compound	κ_a (tan δ)	κ_c (tan δ)	$\langle \kappa' \rangle$	V_m^a (\AA^3)	Frequency	α_D^b (\AA)	Reference
CaO	11.95		11.95		1 MHz	5.22	9
SrO	14.5		14.5			6.48	30
Al ₂ O ₃	9.395	11.589	10.126		1 KHz	7.627	31
Y ₂ O ₃	11.4		11.4		100 KHz	13.81	32
Nd ₂ O ₃						16.3 ^c	This work
La ₂ O ₃					1 MHz	17.7	11
CaYAlO ₄	21.44 ± 0.02 0.0008	16.12 ± 0.04 0.0008	19.67	78.88	1 MHz	16.2	This work
CaNdAlO ₄	19.65 ± 0.1 0.0002	17.65 ± 0.1 0.0004	18.98	82.30	1 MHz	16.8	This work
SrLaAlO ₄	16.81 ± 0.1 0.0006	20.02 ± 0.1 0.0008	17.88	89.15	1 MHz	18.07	This work

^a V_m , molar volume.

^b $\alpha_D = (3/4\pi)(V_m) \cdot (\kappa' - 1)/(\kappa' - 2)$.

^c Obtained from $\alpha_{\text{tot}} = \sum (\alpha_{\text{oxides}})$, where $\alpha_D(\text{NdP}_5\text{O}_{14}) = 39.24 \text{ \AA}^3$ (13), $\alpha_D(\text{Nd}_{3.01}\text{Ga}_{4.99}\text{O}_{12}) = 46.40 \text{ \AA}^3$ (11), $\alpha_D(\text{P}_2\text{O}_5) = 12.44 \text{ \AA}^3$ (13), and $\alpha_D(\text{Ga}_2\text{O}_3) = 8.80 \text{ \AA}^3$ (11).

the other hand the axial Al–O2 distance is determined by both the *c*-cell parameter and a variable *z*-positional parameter; both of these variables will depend on the average ionic radius of the alkaline earth and rare earth cations, since these are disordered

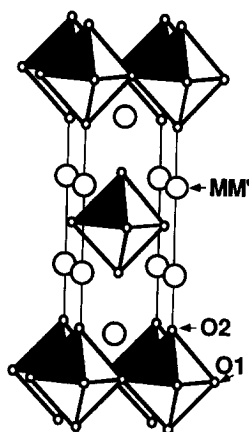


FIG. 1. Polyhedral representation of the structure of the MM' AlO₄ materials ($MM' = \text{CaY}, \text{CaNd}, \text{or SrLa}$). The unit cell is outlined. Al is located at the unit cell corners and center.

over the MM' -cation sites in the ideal K_2NiF_4 -type structure. These is illustrated in Fig. 2, where individual and average Al–O distances, normally relatively invariant, increase regularly with the increase in average size of the MM' cation (Table III), reaching the ideal average value only for SrLaAlO₄. The unusual behavior of the Al–O distances is perhaps better evaluated

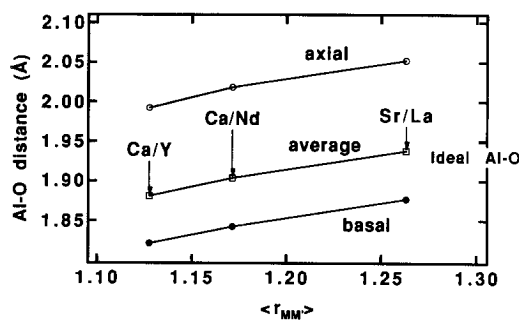


FIG. 2. Variation of the basal, axial, and average Al–O bond distances with the average ionic radius of the MM' cations; radii are taken from Ref. (26). The ideal Al–O distance is calculated from the sum of the ionic radii for 6-coordinated Al^{3+} and O^{2-} .

TABLE V
COMPARISON OF OBSERVED AND PREDICTED SINGLE-CRYSTAL DIELECTRIC POLARIZABILITIES

Compound	$\langle \kappa' \rangle$	Predicted α_T (oxide rule)	Measured $\alpha_T(\text{exp})^a$	$\Delta\%$	$V_{(MM')^b}$	V_{Al}^b
CaYAlO ₄	19.67	15.94	16.22	+1.7	2.35	3.32
CaNdAlO ₄	18.98	17.18	16.84	-2.0	2.36	3.13
SrLaAlO ₄	17.88	19.14	18.07	-5.9	2.58	2.85

^a Using the Clausius–Mosotti relationship; polarizabilities are in cubic angstroms.

^b From Table III.

using bond valences, V_{Al} , calculated from the Brown and Altermatt (27) parameters given in Table III. Table V shows that in CaYAlO₄ and CaNdAlO₄, $V_{Al} > 3$, suggesting compressed Al ions, and in SrLaAlO₄, $V_{Al} < 3$, suggesting slightly expanded Al ions.

As the mean Al–O bond distance increases, the mean MM' –O distance also increases, consistent with the increasing average ionic radii of MM' (Table III). The deviation of these MM' –O distances from those predicted from the ionic radii listed in Table III increases progressively as the average size of the MM' cation increases, suggesting that as the average MM' cation size increases, the Al–O network cannot expand sufficiently to satisfy the bonding requirements of the MM' cations. In terms of bond valence, $V_{MM'}$ increases gradually from less than the ideal value of 2.5 for CaYAlO₄ and CaNdAlO₄, to greater than 2.5 for SrLaAlO₄, (Table V), indicating rattling CaY and CaNd cations and compressed SrLa cations.

Table V compares the total molecular dielectric polarizabilities determined from the measured dielectric constants using the Clausius–Mosotti relationship,

$$\alpha_D = \frac{3}{4\pi} (V_m) \cdot \frac{\kappa' - 1}{\kappa' - 2},$$

where V_m = molar volume and κ' = dielectric constant at 10^5 – 10^{10} Hz and from the

oxide additivity rule. The deviations (Δ) of the observed dielectric polarizabilities of CaYAlO₄, CaNdAlO₄, and SrLaAlO₄ from those calculated from the sum of oxide polarizabilities according to the oxide additivity rule is larger than the typical 1% observed for well-behaved oxides (10). There is a gradual trend of Δ from slightly (+) values for CaYAlO₄ to strongly (–) values for SrLaAlO₄. This trend is accompanied by an increase in mean Al–O distance of 1.878 Å in CaYAlO₄ to 1.935 Å in SrLaAlO₄. This trend in Δ is similar to that observed in the silicate garnet family, $X_3Al_2Si_3O_{12}$, where pyrope garnet ($M = \text{Mg}$) showed a large (+) deviation and grossular garnet ($M = \text{Ca}$) showed a large (–) deviation. A further similarity between the K_2NiF_4 -type aluminates and the silicate garnets is the variation of the normally invariant mean Al–O distance; $d(\text{Al–O})$ for pyrope was found to be 1.886 Å, whereas for grossular it is 1.924 Å (35). In the case of the garnets, an explanation for the trend in Δ could be found in longer than normal Mg–O distances and shorter than normal Ca–O distances which occur because the size of the X site produced by the $Al_2Si_3O_{12}$ framework is constrained by the framework. The effect was more evident from bond valences calculated using the parameters of Brown and Altermatt (27), where V_{Mg} and V_{Ca} were calculated to be 1.72 and 2.52 v.u., respectively, compared to the ideal value of 2.0 v.u.

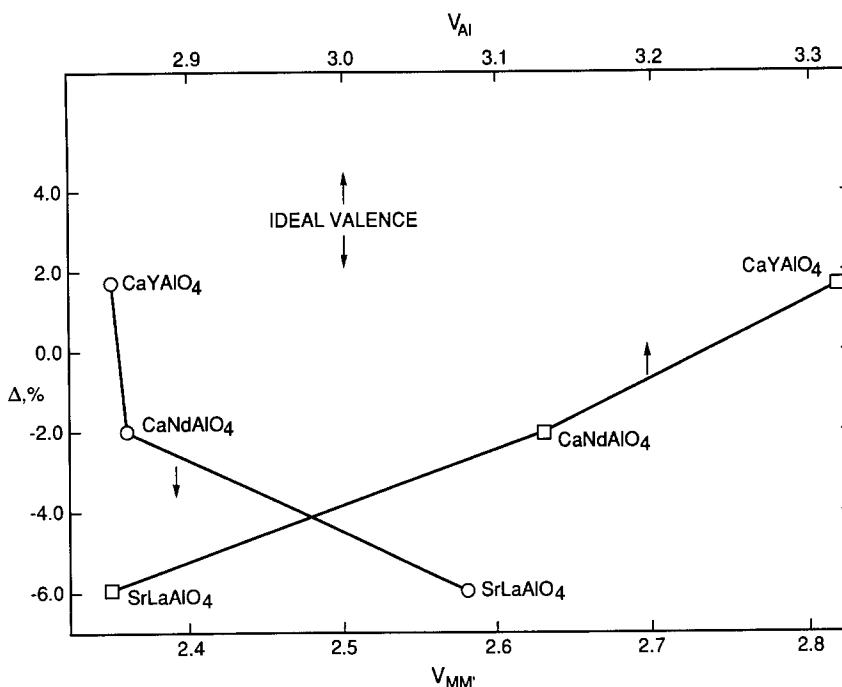


FIG. 3. Deviation from the oxide additivity rule, Δ , vs the apparent bond valence of MM' ($V_{MM'}$) and of Al (V_{Al}).

Similar behavior occurs in the $MM'AlO_4$ compounds. CaYAlO_4 with rattling MM' shows a (+) deviation, whereas SrLaAlO_4 with compressed MM' leads to a (-) deviation. Apparently, the effects of MM' are greater than those of Al because CaYAlO_4 , with rattling MM' and compressed Al, shows a (+) deviation while SrLaAlO_4 , with compressed MM' and rattling Al, shows a (-) deviation. CaNdAlO_4 is an intermediate case. Based on the above argument expanded MM' should lead to (+) deviations. However, it shows a (-) deviation and evidently more complex behavior. These effects are shown graphically in Fig. 3 with the tendency of MM' to fit more loosely in the framework directly opposing the effect of Al being progressively more compressed.

Acknowledgments

We thank R. W. Shiffer for sample preparation, P. K. Carpenter, J. T. Armstrong, and G. R. Rossman for the electron microprobe analyses, C. Foris for obtaining cell dimensions of CaYAlO_4 and SrLaAlO_4 , and W. J. Marshall for assistance with the single-crystal X-ray diffraction study; J.B.P. is grateful for the financial support of the DuPont Company; R.S. thanks the Air Force Office of Scientific Research for partial financial support.

References

1. A. HEYDWEILLER, *Z. Phys.* **3**, 308-317 (1920).
2. C. K. CHENG, *Philos. Mag.* **30**, 505-515 (1940).
3. G. H. JONKER AND J. H. VAN SANTEN, *Chem. Weekbl.* **43**, 672-679 (1947).
4. R. ROBERTS, *Phys. Rev.* **76**, 1215-1220 (1949).
5. R. ROBERTS, *Phys. Rev.* **77**, 258-263 (1950).
6. R. ROBERTS, *Phys. Rev.* **81**, 865-868 (1951).
7. A. C. LASAGA AND R. T. CYGAN, *Am. Mineral.* **67**, 328-334 (1982).

8. R. D. SHANNON, M. A. SUBRAMANIAN, A. M. MARIANO, AND G. R. ROSSMAN, "Proceedings, Material Research Society Symposium," Vol. 150, Materials for Magneto Optic Data Storage" (C. J. Robinson, T. Suzuki, and C. M. Falco, Eds.), April 17 (1989).
9. R. D. SHANNON AND M. A. SUBRAMANIAN, *Phys. Chem. Miner.* **16**, 747-751 (1989).
10. R. D. SHANNON, "Proceedings, International Conference on the Chemistry of Electronic Ceramic Materials," NIST Special Publication 804, pp. 457-471 (1991).
11. R. D. SHANNON, M. A. SUBRAMANIAN, T. H. ALIK, H. KIMURA, M. R. KOKTA, AND G. R. ROSSMAN. *J. Appl. Phys.* **67**, 3798-3802 (1990).
12. R. D. SHANNON, M. A. SUBRAMANIAN, S. HOSOYA, AND G. R. ROSSMAN. *Phys. Chem. Miner.* **18**, 1-6 (1991).
13. R. D. SHANNON, M. A., SUBRAMANIAN, A. N. MARIANO, T. E. GIER, AND G. R. ROSSMAN. *Am. Mineral.* **77**, 94-100 (1992).
14. M. A. SUBRAMANIAN AND R. D. SHANNON, *Mater. Res. Bull.* **24**, 1477-1483 (1989).
15. R. D. SHANNON, AND G. R. ROSSMAN, *Am. Mineral.* **77**, 101-106 (1992).
16. R. SOBOLEWSKI, P. GIERLOWSKI, W. KULA, S. ZAREMBINSKI, S. J. LEWANDOWSKI, M. BERKOWSKI, A. PAJACZKOWSKA, B. P. GORSHUNOV, D. B. LYUDMIRSKY, AND O. I. SIROTINSKY. *IEEE Trans. Magn.* **27**, 876-879 (1991).
17. R. BROWN, V. PENDRICK, D. KALOKITIS, AND B. CHAI, *Appl. Phys. Lett.* **57**, 1351-1353 (1990).
18. Z. S. APPEN, A. Y. VALTERE, L. S. VOROTILOVA, R. M. RAKHMANKULOV, A. Y. ROMANOV, Y. P. UDALOV, AND T. Y. CHEMEKOVA, *Inorg. Mater.* **21**, 716-718 (1985).
19. Z. S. APPEN, A. Y., VALTERE, A. M. KOROVKIN, R. M. RAKHMANKULOV, A. Y. ROMANOV, AND Y. P. UDALOV, *Inorg. Mater.* **21**, 1808-1810 (1985).
20. M. BERKOWSKI, A. PAJACZKOWSKA, P. GIERLOWSKI, S. J. LEWANDOWSKI, R. SOBOLEWSKI, B. P. GORSHUNOV, G. V. KOZLOV, D. B. LYUDMIRSKY, O. I. SIROTINSKY, P. A. SALTYKOV, H. G. SOLTNER, U. POPPE, CH. BUCHTAL, AND A. LUBIG *Appl. Phys. Lett.* **57**, 632-635 (1990).
21. P. BYSZEWSKI, A. PAJACZKOWSKA, J. SASS, AND K. MAZUR, "Proceedings, 3rd European Conference on Crystal Growth—Budapest, Hungary," Transcripts of Technical Publication Ltd., Zurich (1991).
22. J. T. ARMSTRONG in "Microbeam Analysis" (K. J. F. Heinrich, Ed.), pp. 175-180, San Francisco Press, San Francisco (1982).
23. J. T. ARMSTRONG in "Microbeam Analysis—1988" (D. E. Newbury, Ed.), pp. 239-256, San Francisco Press, San Francisco, (1988).
24. P. BYSEZEWSKI, R. DIDUSZKO, J. WOJCIK, AND A. PAJACZKOWSKA. "Proceedings, 3rd European Conference on Crystal Growth—Budapest, Hungary," Transcripts of Technical Publication Ltd., Zurich (1991).
25. J. C. CALABRESE, personal communication.
26. R. D. SHANNON, *Acta Crystallogr. A* **32**, 751-767 (1976).
27. I. D. BROWN AND D. ALTERMATT, *Acta Crystallogr. B* **41**, 244-247 (1985).
28. M. A. SUBRAMANIAN, R. D. SHANNON, B. H. T. CHAI, M. M. ABRAHAM, AND M. C. WINTERSGILL, *Phys. Chem. Miner.* **16**, 741-747 (1989).
29. Hewlett-Packard, "Operating Manual for 4275A Multi-Frequency LCR Meter," Yokogawa-Hewlett-Packard Ltd., Tokyo (1984).
30. R. A. BARTELS, J. C., KOO, AND M. L. THOMAS, *Phys. Status Solidi A* **52**, K213-K216 (1979).
31. J. FONTANELLA, C. ANDEEN, AND D. SCHUELE, *J. Appl. Phys.* **45**, 2852-2854 (1974).
32. W. B. WESTPHAL AND A. SILS, "Dielectric Constant and Loss Data," AFML-TR-72-39, U.S. National Technical Information Service (1972).
33. C. Y. CHEN, R. J. BIRGENEAU, D. R., GABBE, H. P. JENSSEN, M. A. KASTNER, P. J. PICONE, N. W. PREYER, AND T. THIO, *Physica C* **162**, 1031-1032 (1989).
34. D. REAGOR, E. AHRENS, S. W. CHEONG, A. MIGLIORI, AND Z. FISK. *Phys. Rev. Lett.* **62**, 2048-2051 (1989).
35. G. A. NOVAK AND G. V. GIBBS, *Am. Mineral.* **56**, 791-825 (1971).